

The impact absorption effect of the base in drop hammer test assemblies

Mitsuo Izumo^{*†}, Mieko Kumasaki^{**}, and Mitsuru Arai^{***}

^{*}Department of Chemical System Engineering, School of Engineering, the University of Tokyo, 7-3-1 Hongo, Bunkyo-ku, Tokyo 113-8656, JAPAN
Phone : +81-90-9834-1443

[†]Corresponding author : m-izumo@nifty.ne.jp

^{**}Department of Safety Engineering, Yokohama National University, 79-7 Tokiwadai, Hodogaya-ku, Yokohama Kanagawa 240-8501, JAPAN

^{***}Environmental Science Center, the University of Tokyo, 7-3-1 Hongo, Bunkyo-ku, Tokyo 113-0033, JAPAN

Received : October 29, 2015 Accepted : July 26, 2016

Abstract

A drop hammer test of cyclotrimethylene-trinitramine (RDX) was conducted with assemblies that were designed to have an absorber placed under the anvil cylinder. Video images showed that the sample particles ignited after crushing. A polypropylene (PP) plate absorbed the impact from the drop hammer and allowed the median drop-height $H_{50\%}$ for the RDX sample to increase by 2.8 times compared to the result without a plate. This result demonstrates the effect of the condition of the installation and the structure of the base. It also implies the possibility of further development in impact sensitivity testing, providing a better resolution for high-sensitivity explosives.

Keywords : RDX, impact sensitivity, drop hammer, base, absorber

1. Introduction

The number of new chemicals is growing rapidly. It is important to assess their potential risk for explosion in case of an unexpected disaster¹⁾. Sensitivity is also important for the use of explosives. It is expressed by the response to external stimuli. The response mechanisms are complicated, especially those resulting from mechanical stimuli, such as impact or friction. The response is affected by the chemical structures, the surface conditions, the shape of the substance, etc. Although energy applied by mechanical stimuli is mainly converted into heat in explosives, and the heat in turn triggers the explosion, mechanical sensitivity has yet to be fully explained in terms of thermal properties, despite many attempts to do so²⁾⁻⁴⁾. A general rule for how to estimate mechanical sensitivity that is applicable to all chemicals has thus far not been found. Therefore, tests to measure mechanical sensitivity are still practically applied in industry.

The drop hammer test has been widely used for

measuring one type of mechanical sensitivity of explosives, namely the impact sensitivity. Some countries have developed their own test assemblies and methodology. The drop hammer (fall-hammer) test was developed at Federal Institute for Materials Research and Testing (BAM) in Germany, and has been widely used for testing both solid and liquid substances^{5),6)}. In Japan, drop hammer test assemblies and methodology have been stipulated by Japanese Industrial Standards. These tests determine the smallest impact energy for a sample to cause at least one "explosion" in six trials. The smallest height that triggers ignition serves as a parameter for the mechanical sensitivity, and helps to judge whether the substance is too dangerous to handle. However, it is usually difficult to obtain a clear boundary between the regions where the energy is sufficient and insufficient to cause explosion.

To overcome these difficulties, the Bruceton method is often used⁷⁾. In this method, the drop hammer test produces a series of trials whose result can be classified as

either “go” (ignition) or “no go” (no ignition). The probability of each result occurring changes gradually as the height of the hammer and the impact changes. Many substances do not show a clear boundary between energies causing “go” and energies resulting in “no go” in a sequence of trials. However, their sensitivity is expressed by the percentage of “go” and “no go”. In many cases, the hammer height resulting in 50% “go” results is used as the index representing sensitivity, which is called the median drop height $H_{50\%}$.

The median drop height $H_{50\%}$ is not a constant value for each substance. The structure of the test assemblies affects the test results and the value of $H_{50\%}$. Variations between assemblies are not negligible in comparing $H_{50\%}$ values obtained with different assemblies. The energy from the drop hammer is not fully applied to the sample. It is partially absorbed and turns into heat because of insufficient hardness of the anvil⁸⁾. One option for gaining universal parameters is to use the ratio of the sample's $H_{50\%}$ to the $H_{50\%}$ of a standard explosive. This value is called the figure of insensitiveness (F. I.), which eliminates variations between assemblies⁷⁾. Proper parameters for ignition by a drop hammer have also been discussed. In many cases, transition of momentum during impact is adopted as a more appropriate parameter than the potential energy of the drop hammer.

Dried cyclotrimethylene-trinitramine (RDX, $C_3H_6N_6O_6$) is used as a standard explosive for this purpose⁶⁾. RDX can explode from only 5 J of impact energy, which is almost equal to the potential energy of a 5 kg hammer dropped from 10 cm height. More sensitive explosives, for example, lead (II) azide ($Pb(N_3)_2$), explode in almost all cases when a hammer is dropped from 5 cm height. Such a high sensitivity is a hindrance to yielding “no go” results and determining $H_{50\%}$. Five-kilogram drop hammer assemblies limit the range between 5 cm and 100 cm (2.45–49.0 J). In order to generate a proper $H_{50\%}$ value for extremely sensitive materials, the impact should be weakened. Two approaches can make the impact weaker: reducing the drop-hammer weight, or absorbing the impact of the drop hammer.

This report sheds light on the latter approach by absorbing the impact through the base. The anvil settings were designed to place an absorber under the cylinder. By employing RDX the effect of the absorber was verified, to determine if the settings can provide higher resolution for measuring ignition energies of highly sensitive explosives. Photographic images were taken to prove that the impact was properly applied to the sample. Single particles were employed for the experiments to avoid using powder since usually the amount of powder employed for sensitivity tests is greater than a single particle. As powder is more commonly used for drop-hammer test, the results of single-particle and powder RDX were compared.

2. Experimental

2.1 Drop hammer test assemblies

Figure 1 is a sectional drawing of the base part in the drop hammer test assemblies. The base supporting the

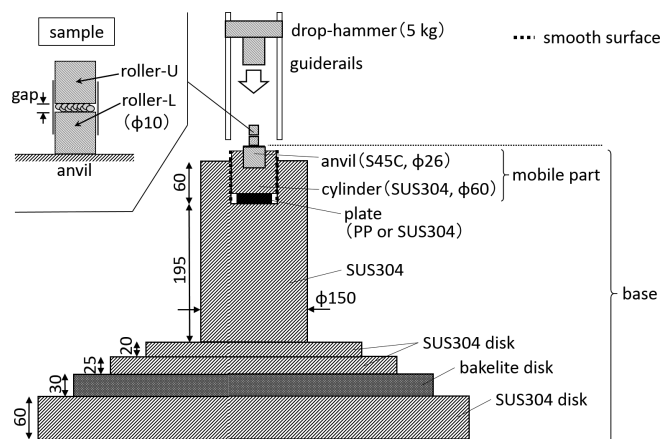


Figure 1 Schematic drawing of drop hammer test assemblies.

anvil had cylindrical symmetry. The disc-shaped bases were mounted together with screws. The anvil (made from S45C steel, diameter 26 mm) and the cylinder (made from SUS304, diameter 60 mm) were attached to each other and moved together (mobile part). The mobile part weighed 1.34 kg. The gap between the mobile part and the cylinder base allowed an absorber to be placed.

The five-kilogram hammer dropped along rails fixed separately from the base. Collisions of the hammer and the roller were recorded with an HPV-1 camera (Shimadzu Corp.) every 64 μs (15,625 frames per second). This camera was used to check the hit position, and to determine the speed of each item in the assembly. Each recording was started by a triggering signal from a photoelectric switching sensor E3T-CT22 (OMRON Corp.), which was positioned 20 cm above the anvil surface.

Prior to the tests with explosives, photo images tracked the movement of the hammer and two rollers to confirm that the hammer hit the roller-U properly. The recorded velocity of the hammer at time of collision was 84.5% of the theoretical free-fall velocity. As the speed reduction may have been caused by friction between the rails and the hammer, the corrected height h applying the same amount of impact as the tests is given by:

$$h = 0.845 h' \quad (1)$$

where h' is the measured height from the upper surface of the roller-U to the bottom of the hammer. This height depends on the type of test and is not affected by the gap width between the mobile part and the cylinder base.

Figure 2 shows the sample setting and roller configurations in the tests. Two types of samples were compared to each other with the assemblies: single particle and powder. Alignment A and A* are for a single particle, alignment B is for powders. The sample settings for powder correspond to the tests standardized by BAM, apart from the confinement with adhesive tape. Samples were placed between the rollers with a radius of 5 mm. Adhesive tape was wound around rollers once. This tape was made of cellophane and its thickness was 0.05 mm. The surface of rollers was cleaned using acetone and dried before tests. Tests were carried out at atmospheric conditions. For powder testing, each trial used 40 mm³ of

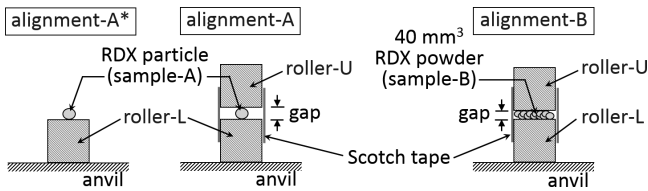


Figure 2 Sample alignment for three test types.
*Gap interval of alignment-A depends on particle size (1.0–3.0 mm). Gap interval of alignment-B is around 0.8 ± 0.2 mm.

the powder, which was placed onto the roller without pressing. Its apparent density was estimated to be 0.72 g cm^{-3} and the void fraction was around 60 %.

Three types of tests, A1-A3, were conducted depending on the condition of the gap between the mobile part and the base: a polypropylene (PP) plate (test A1), a steel (SUS) plate (test A2), and no plate (test A3). The thicknesses of the PP plate and the SUS plate were 20 mm and 15 mm, respectively.

2.2 Sample preparation

α -RDX was employed as the sample. For recrystallization, RDX (class A, made by Nippon Koki Co., Ltd.) was dissolved into anhydrous acetone, and the acetone was partially evaporated at room temperature to recrystallize RDX particles. For these tests, particles ranging 1.20–3.02 mm in diameter were used (sample A). Figure 3 is a picture of a typical sample A.

Sample A was crushed with a pestle. Powder was separated from the remaining particles. This powder was sample B. Figure 4 shows the particle size distribution of sample B, showing a median size of 0.308 mm. The water content of sample B was $0.99 \pm 0.17\%$, measured by Karl Fischer titration⁹. RDX is known to become slightly

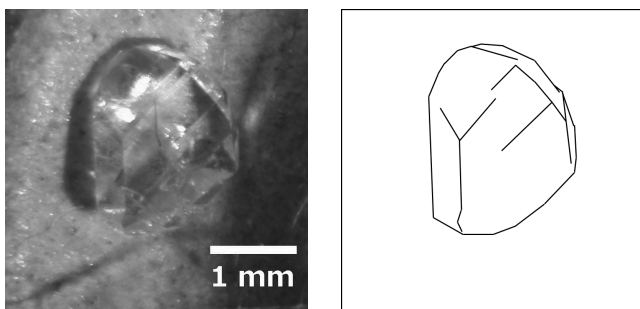


Figure 3 Microscopic picture of typical RDX sample A. The extracted edges of the particle were drawn on the right.

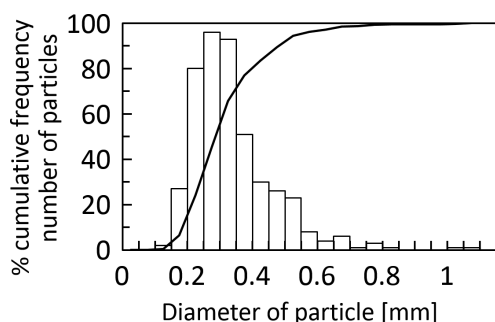


Figure 4 Size distribution of RDX sample-B.

Table 1 The criteria of “go” or “no go” (common with alignment A and B).

“go”	RDX has disappeared and traces are left on the roller.
“no go”	RDX is left on the roller.

insensitive when its water content exceeds 0.10%^{10,11}. The water in the sample was well-controlled, however it might affect the sensitivity.

2.3 The procedure to calculate $H_{50\%}$ as the index of sensitivity

Each test was conducted according to the Bruceton method⁷, which produces $H_{50\%}$. In the method, the hammer is dropped from a series of heights at identical logarithmic intervals: $h' = 7, 10, 14, 20, 28, 40, 56, \text{ and } 80$ cm. After the impacts, the results were judged “go” or “no go” based on the criteria listed in table 1. All experiments with RDX provided clear results. More than 40 trials were conducted to obtain each data series.

When “go” and “no go” are designated as 1 and 0, respectively, the average of the data gives the explosion probability. This probability is considered to increase as the energy or drop height increases, and the probability can be expressed as a curve versus the impact energy or drop height. This curve is another expression of sensitivity, taking the intermediate region between “go” and “no go” into account.

Assuming that the distribution of the “go” and “no go” threshold boundaries for each sample can be described by the Gauss function (Equation 2), the cumulative distribution is given by Equation 3. The cumulative distribution expresses a left-side section integral of Equation 2. The unit of height h is cm and $h\sqrt{2\pi\sigma^2}$ is a value for normalizing.

$$f(h) = \frac{1}{h\sqrt{2\pi\sigma^2}} \exp\left(-\frac{(\log_{10} h - \mu)^2}{2\sigma^2}\right) \quad (2)$$

$$P(h) = \frac{1}{\sqrt{2\pi\sigma^2}} \int_0^h \frac{1}{x} \exp\left(-\frac{(\log_{10} x - \mu)^2}{2\sigma^2}\right) dx \quad (3)$$

$P(h)$ increases smoothly from 0 to 1, and the values of μ (average) and σ (standard deviation) were optimized to fit the experimental data. The parameters were determined by the method of maximum likelihood¹². The parameter μ corresponds to the median drop-height $H_{50\%}$ and σ^2 is a measure of the variance of the sample threshold between “go” and “no go”.

3. Result and discussion

3.1 Observation of the compression and the ignition process

Figure 5 shows photographic images tracking the movement of the rollers triggered by the impact of the hammer dropped from 56 cm height. In figure 5(b), 5(c) and 5(d), numbers on the right side of each image indicate “elapsed time” from when the edge of the hammer reached the upper end of a particle or roller. Because the

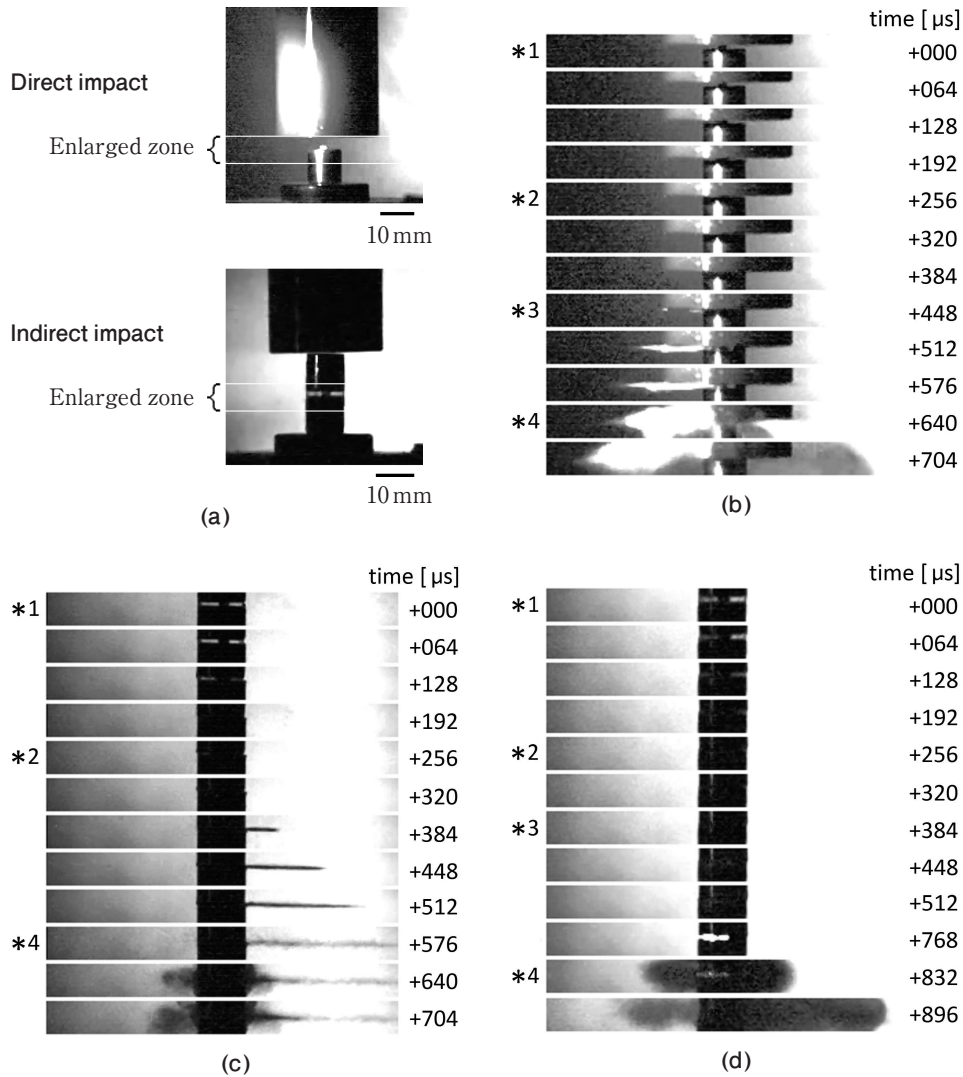


Figure 5 Initiation of single particle RDX.
 (a): pictures before impact and enlarged area.
 (b): time-series pictures during direct impact (alignment A*)
 (c): time-series pictures during indirect impact (alignment A, with ejection)
 (d): time-series pictures during indirect impact (alignment A, without ejection) Annotation in (b)–(d)
 *1 : compression started, *2 : the gap disappeared, *3 : ejection started, *4 : ignition started.

buckling stress of the adhesive tape is much smaller than the impact force applied by the hammer, the effect of the tape could be ignored. As a result, the setup allowed the impact to be applied to samples adequately by the video images. During the impact, the gap between rollers was narrowed in alignment A.

Prior to ignition of a particle sample, a compression process without ignition was found with a range of 0 to 256 μ s. In this process, the gap became thinner and finally unobservable. The particle was pressed and crushed. In this process, gas ejection blow was observed at 448 μ s in figure 5(b) and at 384 μ s in figure 5(c). Light was emitted a few hundreds of microseconds after compression completed from where the gap used to be. The sample between the rollers ignited and generated gas blowing out again at 832 μ s in figure 5(c) and at 576 μ s in figure 5(d). This ignition blow was clearly different from ejection blow in terms of the rate and direction. The ignition blow is nondirectional and slower than the ejection blow. In the case without ejection, there were a few microseconds after

the gap between rollers disappeared. The video images supported the statement that the particle was crushed into powder before ignition.

The ejection blow was also observed at non-ignited trials. Non-ignited sample with one or a few holes in the tape were found after the trials. These holes indicated that gases penetrated the tape although non-ignited samples was collected. Therefore, these gases were the air existed between rollers.

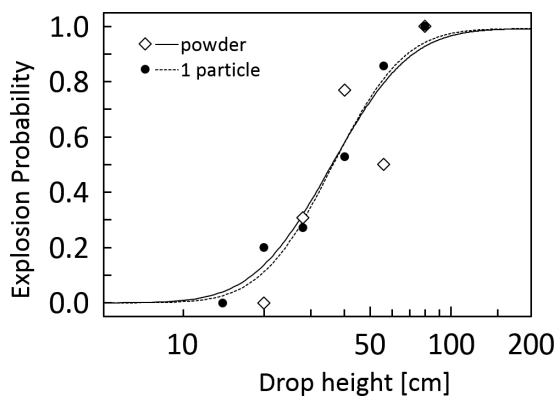
The delayed ignition indicates that the process of ignition is independent from the process of compression. In this study, the particle of RDX was brittle and was crushed into smaller particles at the beginning of compression, which dispersed stress that could cause ignition. In other words, a particle of RDX exploded after it becomes powder. The initial shape of RDX may have little effect on sensitivity. The question then arises whether a particle of RDX ignites at the same impact level as powdered RDX. To answer this question, a series of tests were carried out, which are described in section 3.2.

4
1
2

Table 2 The sample dependence of the impact sensitivity test.

Height h' [cm]	Height h [cm]	$\log_{10} h$	Explosion probability*	
			Sample-A (one particle)	Sample-B (powder)
80	67.5	1.83	1/1	3/3
56	47.3	1.67	6/7	3/6
40	33.8	1.53	9/17	10/13
28	23.7	1.37	3/11	4/13
20	16.9	1.23	1/5	0/4
14	11.8	1.07	0/2	–
fitted μ			1.56	1.56
fitted σ			0.21	0.23
fitted $H_{50\%}$			36 cm	36 cm

* Number shows the number of “go” results in all trials

**Figure 6** Explosion probability and fitted curve $P(h)$.

3.2 Difference between powder RDX and single particle RDX

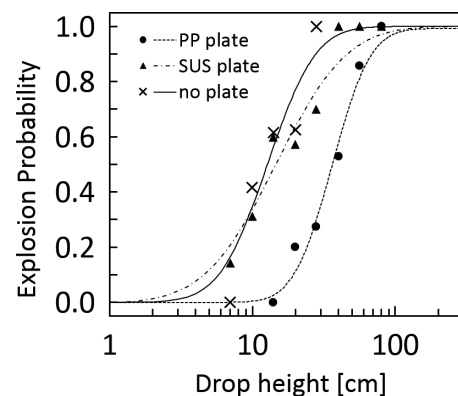
This section verifies the hypothesis that $H_{50\%}$ of a particle and a powder are similar, which was implied from the video images. Sensitivity tests of sample A (one particle sample) and sample B (powder sample) were carried out to compare the effect of particle-particle interaction with assemblies that include an absorber plate. Table 2 contains the dataset of height and explosion probability, which accounts for the number of “go” results in all trials at each drop height. Figure 6 shows the fitted curve $P(h)$, which expresses the explosion probability from table 2. Curves expressed as the formula in Equation 3 are fitted to the data.

The results indicated that an RDX particle ranging 1.2–3.0 mm in diameter behaves almost in the same way as RDX powder. Test alignments A and B gave similar values for the fitting parameters μ and σ . The parameter μ mathematically means the average, and experimentally means the logarithm of the median drop height, $\log_{10} H_{50\%}$. The relationship “ $\mu = 1.56$ ” corresponds to “ $H_{50\%} = 36$ cm”. The parameter σ mathematically means the standard deviation, and experimentally means the deviation of $\log_{10} H_{50\%}$. As such, the similar value of μ indicates that the two alignments gave the same impact sensitivity despite the different sample condition.

Table 3 The effect of absorber plate on impact sensitivity.

Height h' [cm]	Height h [cm]	$\log_{10} h$	Explosion probability*		
			Test A1 (with PP plate)	Test A2 (with SUS plate)	Test A3 (without space)
80	67.5	1.83	1/1	–	–
56	47.3	1.67	6/7	1/1	–
40	33.8	1.53	9/17	1/1	–
28	23.7	1.37	3/11	7/10	3/3
20	16.9	1.23	1/5	8/14	5/8
14	11.8	1.07	0/2	12/20	8/13
10	8.4	0.93	–	5/16	5/12
7	5.9	0.77	–	1/7	0/4
fitted $H_{50\%}$			36 cm	15 cm	13 cm

* Number shows the number of “go” results in all trials

**Figure 7** Explosion probability depending on condition of the base.

The recorded video observed the presence of a delay prior to ignition. The delay covers the crushing of a particle; explosion was detected after the particle was pressed to powder. The results show agreement with the observations.

3.3 The effect of absorber

Table 3 summarizes the dataset obtained from the experiments of single particles of RDX with or without a plate in the assemblies. Figure 7 shows the plots exhibiting explosion probability in table 3 and the fitted curves for $P(h)$ as given by Equation 3. The median values of drop height $H_{50\%}$ were 37 cm for A1, 15 cm for A2, and 13 cm for A3.

The presence of an absorber increased $H_{50\%}$ by 2.8 times. Since PP showed elastic behavior, the hammer impacts were supposed to be absorbed effectively.

All tests were conducted in the same manner and the impact was considered to be transmitted through the RDX particle irrespective of the sample alignment condition. A difference must have emerged after the wave reflected at the bottom of the mobile parts and reached the particle. The waves travel repeatedly between the boundaries and energy builds up leading to explosion. Although the wave first reflected at the absorber is the most effective, the following waves also contribute to the energy. The duration of the energy build-up can be the

cause of the delay between crushing and ignition captured by the video.

The increase of $H_{50\%}$ by 2.8 times corresponds to a broadening of the interval width between drop heights. This change can provide better resolution of experiments for highly sensitive materials.

4. Conclusion

Sensitivity is important information for the use of explosives. This study investigates the approach of absorbing the impact through the base to obtain a better sensitivity resolution for highly sensitive explosives.

The measured $H_{50\%}$ value of RDX was greater with a PP plate under the anvil than with a SUS plate. This result indicates that the configuration of the base significantly affects the measurement of sensitivity data.

Video images of RDX particles whose diameter ranged from 1.2 to 3.0 mm showed that the particles were crushed during impact and that ignition was delayed. In the sensitivity test, the process of ignition was independent from the process of compression under impact.

The drop hammer test can provide better test resolution for high-sensitivity explosives without changing the weight of the hammer if we exploit the arrangement to attenuate the energy of the hammer.

This study can be used to establish a method to distinguish between several highly sensitive explosives with almost equal $H_{50\%}$ and also informs us that sensitivity data should be used with care. Sensitivity data obtained with a fixed setup of assembly, hammer, and bases should be adopted and compared to each other. This study contributes to safe handling and more appropriate material management tailored to each explosive.

Acknowledgement

We thank Dr. Koki Ishikawa, Dr. Eishi Kuroda, and Dr. Yoshio Nakayama for the use of the drop hammer assemblies and cameras. This work was made possible through the help of our laboratory members. These assemblies are installed at the National Institute of Advanced Industrial Science and Technology (AIST).

References

- 1) T. Yoshida, Y. Wada, and N. Foster, "Safety of Reactive Chemicals and Pyrotechnics", Elsevier Science B.V., 22 (1995).
- 2) C.B. Storm, J.R. Stine, and J.F. Kramer, *Chemistry and Physics of Energetic Materials*, 309, 605–639 (1990).
- 3) J.K. Dienes, Q.H. Zuo, and J.D. Kershner, *Journal of the Mechanics and Physics of Solids*, 54, 1237–1275 (2006).
- 4) X.S. Song, X.L. Cheng, X.D. Yang, and B. He, *Propellants, Explosives, Pyrotechnics*, 31 (2006).
- 5) H. Koenen, K.H. Ide, and W. Haupt, *Explosivstoffe*, 6, 178–189, 202–214, 223–235 (1958).
- 6) United Nations, "UN Manual of Tests and Criteria, Recommendations on the Transport of Dangerous Goods", Fifth revised edition, 69–103 (2009).
- 7) W.J. Dixon and A.M. Mood, *Journal of the American Statistical Association*, 43, 109–126 (1948).
- 8) N.R.S. Hollies, N.R. Legge, and John L. Morrison, *Canadian Journal of Chemistry*, 31, 746–754 (1953).
- 9) F. Karl, *Angewandte Chemie*, 48, 394–396 (1935).
- 10) T. Ishizuka and K. Okazaki, *Kogyo Kayaku Kyokaiishi*, (Sci. Tech. Energetic Materials) 34, 86–92 (1973) (in Japanese).
- 11) T. Katsuta and K. Okazaki, *Annual Conference of Industrial Explosives Soc. Japan*, 25 (1969) (in Japanese).
- 12) S.S. Wilks, *Ann. Math. Statist.*, 9, 1, 60–62 (1938).